

Spin polarized photons and dileptons from axially charged plasmaKiminad A. Mamo^{1,*} and Ho-Ung Yee^{1,2,†}¹*Department of Physics, University of Illinois, Chicago, Illinois 60607, USA*²*RIKEN-BNL Research Center, Brookhaven National Laboratory, Upton, New York 11973-5000, USA*

(Received 11 September 2013; published 26 December 2013)

Axial charge in a QCD plasma is P- and CP-odd. We propose and study P- and CP-odd observables in photon and dilepton emissions from an axially charged QCD plasma, which may provide possible experimental evidences of axial charge fluctuation and triangle anomaly in the plasma created in heavy-ion collisions. Our observables measure spin alignments of the emitted photons and dileptons, and are shown to be related to the imaginary part of chiral magnetic conductivity at finite frequency-momentum, which ultimately arises from the underlying triangle anomaly of the QCD plasma with a finite axial charge density. We present an exemplar computation of these observables in a strongly coupled regime using AdS/CFT correspondence.

DOI: 10.1103/PhysRevD.88.114029

PACS numbers: 12.38.Mh, 13.88.+e, 11.30.Er

I. INTRODUCTION

Triangle anomaly (or chiral anomaly) of the axial symmetry in QCD with (nearly) massless quarks is a result of an interesting quantum mechanical interplay between spins, helicities and charges of the fundamental fermionic constituents of the matter we observe in the Universe. It dictates that the axial current conservation, which naively holds true in the classical limit, is violated quantum mechanically by¹,

$$\partial_\mu J_A^\mu = \frac{e^2}{2\pi^2} \vec{E} \cdot \vec{B}, \quad (1.1)$$

in the presence of a P- and CP-odd environment provided by a nonzero $\vec{E} \cdot \vec{B}$. Its physics consequences are rich, in both low and high temperature/density phases of QCD matter, and quite recently a lot of interests have been attracted to some of its effects in a high temperature quark-gluon plasma created in heavy-ion collisions and their possible experimental observations, which could be one of the direct experimental tests of the fundamental symmetries of QCD.

One such phenomenon is the chiral magnetic effect (CME) [1–5] which dictates the existence of an electromagnetic current in the presence of a background magnetic field,

$$\vec{J}_{\text{EM}} = \frac{e^2 \mu_A}{2\pi^2} \vec{B}, \quad (1.2)$$

where μ_A is the axial chemical potential. It should be emphasized that the above result is valid in the zero

momentum limit, $(\omega, k) \rightarrow 0$, and one can introduce frequency dependent chiral magnetic conductivity at finite ω [6]. In off-central heavy-ion collisions, the ultrarelativistic heavy-ion projectiles can create a huge magnetic field which provides an ideal setup for CME [2], and the axial charges may be created event-by-event either by the glasma color fields in the early stage of collisions or by thermal sphaleron transitions in a later stage [2,7,8]. The induced event-by-event charge separation from the CME may lead to some experimental signatures [9] that indeed seem to be consistent with the observations in RHIC [10] and LHC [11]. However, as the proposed signal is roughly the square of the charge separations in order to avoid event-averaging to zero, the signal is in fact P-even and may get additional contributions from other background effects unrelated to triangle anomaly [12–15], which makes it hard to draw definite conclusions on the CME in heavy-ion collisions.

Another related phenomenon is the chiral magnetic wave (CMW) [16,17] which is a gapless soundlike propagation of chiral (that is, left-handed or right-handed) charges along the direction of the magnetic field. The CMW may lead to a nonzero electric quadrupole moment in the plasma fireball [18–20] that can explain the experimentally observed [21,22] charge-dependent elliptic flows of pions at RHIC [19,20]. Although this is quite suggestive to the existence of the phenomenon, similarly to CME the observable is sensitive to other background effects not originating from triangle anomaly [23–27].

It is desirable to have some observables which are direct consequences of triangle anomaly, yet without having contributions from other backgrounds that have nothing to do with triangle anomaly. A promising direction is to use discrete symmetries, that is, parity (P) and charge conjugation (C) transformations, to identify such observables, since the axial charge and the triangle anomaly is P- and CP-odd which is a unique characterization of

*kabebe2@uic.edu

†hyee@uic.edu

¹This is the covariant form of anomaly with a single Dirac fermion of charge e .

its physics effects. As these discrete symmetries are exact in QCD, any P- and CP -odd observable would be a direct consequence of axial charge fluctuations and the triangle anomaly.

As a first step in this direction, we study possible P- and CP -odd observables in the photon and dilepton emission rates from a quark-gluon plasma. Since QCD as a theory is P- and CP -even, these observables are necessarily based on event-by-event P- and CP -odd fluctuations of axial charges. However, photons and dileptons are relatively cleaner observables than the hadrons, so our observables may have some potential to be experimentally measurable event-by-event.

Our P- and CP -odd observables for photons and dileptons from an axially charged plasma are essentially spin alignments along the momentum direction which measure the net helicity of the photons and dileptons. Since the axial charge is nothing but the helicity asymmetry of the fermionic quasiparticles of the plasma², our observables measure how such fermionic helicity is reflected to the helicities of the emitted photons and dileptons. We will see that our observables are proportional to the imaginary part of the chiral magnetic conductivity $\sigma_\chi(\omega, k)$ at finite frequency-momentum, defined by a P- and CP -odd part of the retarded current-current correlation functions [6]

$$G_{ij}^{R,-} = i\sigma_\chi(\omega, k)\epsilon_{ijk}k^k, \quad i, j, k = 1, 2, 3, \quad (1.3)$$

which is well known to be a consequence of triangle anomaly. Note that $\sigma_\chi(\omega, k)$ is the coefficient of the CME at finite frequency-momentum,

$$\vec{J}_{EM} = e^2\sigma_\chi(\omega, k)\vec{B}(\omega, k), \quad (1.4)$$

treating the magnetic field as a linear perturbation with a finite frequency-momentum. Hence, our observables are the direct tests of the existence of triangle anomaly in QCD.

We emphasize that our observables are not based on the presence of external electromagnetic fields such as the magnetic field in CME/CMW, nor on the geometric flows and anisotropies, and only assume the existence of axial charge fluctuations³. Since the typical relaxation time scale of axial charges in the RHIC plasma is about ~ 1 – 10 fm depending on α_s , (and larger for LHC with a smaller α_s) [40], the sign of the net axial charge in a fireball can be coherent event-by-event, and our observables may well be nonzero event-by-event.

²See Ref. [28] for an interesting exact relation between fermionic helicity and the axial chemical potential.

³The possible effects of the magnetic field to the photon emission rate, explaining the measured elliptic flow [29,30], have been discussed in Refs. [31–39].

An interesting observation on the effect of triangle anomaly to the photons interacting with the plasma was previously made in Ref. [41], showing that the photon field with a particular polarization is unstable and seems to grow. The physics is based on the same P- and CP -odd part of the retarded correlation functions (1.3), now entering the dispersion relation of a photon field interacting with the plasma medium. Although this is quite interesting, for this instability to be realized, the time scale should be long enough to allow multiple interactions between photons and the plasma. Due to a smallness of electromagnetic coupling $\alpha_{EM} \ll 1$, this required time scale is parametrically long (proportional to α_{EM}^{-1}), and based on this, it has been typically assumed that the photons in heavy-ion collisions once emitted from the plasma do not interact with the plasma again before they leave out the fireball, and the well-known photon emission rate is based on this premise. In this case, the more plausible phenomenon happening in real heavy-ion collisions seems to be a simple asymmetry in the emission rates for different spins we discuss.

II. P- AND CP -ODD OBSERVABLES

The axial charge in the QCD plasma is a P- and CP -odd quantity, and the experimental signatures from the axially charged plasma should naturally feature some of P- and CP -odd observables. In this section, we identify such observables in photon and dilepton emissions, whose experimental measurements may serve as definitive evidences of the existence of axial charges in the plasma created in heavy-ion collisions. Since these observables naturally involve P- and CP -odd part of the charge current correlation functions which is one of the consequences of the underlying axial-vector-vector triangle anomaly, their observation would also be a direct evidence of triangle anomaly in QCD.

A. Photons

Recall that we are considering a homogeneous, isotropic QCD plasma without any external electromagnetic field present. Our only assumption is that the plasma is axially charged, while the vector charge may or may not be present. The axial charge may come from the longitudinal color fields in the early glasma phase, or from thermal sphaleron fluctuations in a later thermalized stage. Since QCD is P- and CP -even (with $\theta_{QCD} = 0$), these axial charge fluctuations can only be nonzero event-by-event. Therefore, our P- and CP -odd observables that we discuss in this work should also be taken as event-by-event observables.

We are interested in P- and CP -odd observables in photon emissions from an axially charged isotropic plasma. Since the plasma is isotropic, let us choose without loss of generality the direction of momentum of the emitted photon to be along x^3 : $\vec{k} = k\hat{x}^3$. What remains is the choice of the polarization of the photon, and it is easy to think of a

P-odd quantity associated with photon polarization, which is the circular polarization of the photon. This is equivalent to the helicity that is whether the unit spin angular momentum of the photon is along or opposite to the direction of the momentum. The corresponding polarization vectors for our choice of momentum vector are

$$\epsilon_{\pm}^{\mu} = (\epsilon^0, \epsilon^1, \epsilon^2, \epsilon^3) = \frac{1}{\sqrt{2}}(0, 1, \pm i, 0), \quad (2.1)$$

where \pm is the helicity of the photon state. In the presence of axial charge which is P- and CP-odd, the natural and simple observable signal of the axial charge is the difference in the photon emission rates between + and - circularly polarized states, and we define ‘‘circular polarization asymmetry,’’

$$A_{\pm\gamma} \equiv \frac{\frac{d\Gamma}{d^3\vec{k}}(\epsilon_+) - \frac{d\Gamma}{d^3\vec{k}}(\epsilon_-)}{\frac{d\Gamma}{d^3\vec{k}}(\epsilon_+) + \frac{d\Gamma}{d^3\vec{k}}(\epsilon_-)}, \quad (2.2)$$

where $d\Gamma/d^3\vec{k}(\epsilon^{\mu})$ is the photon emission rate per unit volume and per unit phase space with a polarization ϵ^{μ} . Since photons are C eigenstates, it is easy to see that $A_{\pm\gamma}$ is P- and CP-odd. In Sec. III, we provide an exemplar model computation of $A_{\pm\gamma}$ in strongly coupled regime, showing that $A_{\pm\gamma}$ is nonzero if and only if an axial charge is present.

To see how $A_{\pm\gamma}$ probes the P- and CP-odd property of QCD plasma which ultimately comes from the underlying triangle anomaly, let us relate $A_{\pm\gamma}$ with the charge current correlation functions by a well-known formula for the photon emission rate,

$$\frac{d\Gamma}{d^3\vec{k}}(\epsilon^{\mu}) = \frac{e^2}{(2\pi)^3 2|\vec{k}|} \epsilon^{\mu}(\epsilon^{\nu})^* G_{\mu\nu}^<(k)|_{k^0=|\vec{k}|}, \quad (2.3)$$

with

$$G_{\mu\nu}^<(k) \equiv \int d^4x e^{-ikx} \langle J_{\mu}(0) J_{\nu}(x) \rangle, \quad (2.4)$$

where J_{μ} is the electromagnetic charge current, and our metric convention is $\eta = (-, +, +, +)$. In the Appendix A, we present a quantum mechanics derivation of (2.3) as a pedagogic exercise, which also clarifies how the polarization vector ϵ^{μ} enters the formula. Relating (2.3) with the retarded correlation functions needs some caution because our polarization vector is complex-valued. Following the steps in Sec. 2 of Ref. [37], we show that the result is

$$\frac{d\Gamma}{d^3\vec{k}}(\epsilon^{\mu}) = \frac{e^2}{(2\pi)^3 2|\vec{k}|} \frac{-2}{e^{\beta|\vec{k}|} - 1} \text{Im}[\epsilon^{\mu}(\epsilon^{\nu})^* G_{\nu\mu}^R(k)]|_{k^0=|\vec{k}|}, \quad (2.5)$$

with the retarded correlation functions

$$G_{\mu\nu}^R(k) \equiv -i \int d^4x e^{-ikx} \theta(x^0) \langle [J_{\mu}(x), J_{\nu}(0)] \rangle. \quad (2.6)$$

Note that the polarization vectors are contracted with the retarded correlation functions first before taking the imaginary values. Using the expression (2.1), the polarization-contracted retarded correlation function takes a form with our choice of the momentum $\vec{k} = k\hat{x}^3$ as

$$\epsilon_{\pm}^{\mu}(\epsilon_{\pm}^{\nu})^* G_{\nu\mu}^R = \frac{1}{2}(G_{11}^R + G_{22}^R \pm iG_{12}^R \mp iG_{21}^R), \quad (2.7)$$

for the \pm polarized states, respectively. Since we have a rotational symmetry in the (x^1, x^2) -plane, the correlation functions along (x^1, x^2) must take a form

$$G_{ij}^R = A\delta_{ij} + B\epsilon_{ij}, \quad i, j = 1, 2, \quad (2.8)$$

which dictates that

$$G_{11}^R = G_{22}^R, \quad G_{12}^R = -G_{21}^R. \quad (2.9)$$

Then, (2.7) simplifies to

$$\epsilon_{\pm}^{\mu}(\epsilon_{\pm}^{\nu})^* G_{\nu\mu}^R = (G_{11}^R \pm iG_{12}^R) \equiv G_{\pm}^R, \quad (2.10)$$

in terms of which the circular polarization asymmetry is written as

$$\begin{aligned} A_{\pm\gamma} &= \frac{\text{Im}G_{+}^R - \text{Im}G_{-}^R}{\text{Im}G_{+}^R + \text{Im}G_{-}^R} \Big|_{k^0=|\vec{k}|} = \frac{\text{Re}G_{12}^R}{\text{Im}G_{11}^R} \Big|_{k^0=|\vec{k}|} \\ &= \frac{2\text{Re}G_{12}^R}{\text{ImTr}G^R} \Big|_{k^0=|\vec{k}|} = \frac{\text{Im}\sigma_{\chi}(k^0)}{\text{Re}\sigma_{11}(k^0)}, \end{aligned} \quad (2.11)$$

where we used $G_{12}^R \sim ik^0\sigma_{\chi}(k^0)$ and $G_{11}^R \sim -ik^0\sigma_{11}(k^0)$ to get the last line. We will find the first expression most useful in practical computations later, while the other expressions show that $A_{\pm\gamma}$ probes a nonvanishing G_{12}^R or a nonvanishing imaginary part of the chiral magnetic conductivity $\sigma_{\chi}(k^0)$.

Since in the zero frequency limit, the chiral magnetic conductivity $\sigma_{\chi}(k^0)$ is given by

$$\lim_{k^0 \rightarrow 0} \sigma_{\chi}(k^0) = \frac{\mu_A}{2\pi^2}, \quad (2.12)$$

which is real, we expect the imaginary part of the chiral magnetic conductivity hence the circular polarization asymmetry $A_{\pm\gamma}$ to vanish in the zero frequency limit of our numerical computation. We also expect the circular polarization asymmetry $A_{\pm\gamma}$ to be proportional to the axial chemical potential μ_A .

The nonvanishing G_{12}^R when the momentum is $\vec{k} = k\hat{x}^3$ is indeed the P- and CP-odd part of the current correlation functions. The only 3D rotationally invariant expression that contributes to G_{12}^R is

$$G_{ij}^R \sim i\sigma_\chi(k)\epsilon_{ijk}k^k, \quad i, j, k = 1, 2, 3, \quad (2.13)$$

which is P- and CP-odd. The coefficient $\sigma_\chi(k)$, called the chiral magnetic conductivity [6], which is in general a function of k^μ , is responsible for the chiral magnetic effect at finite frequency and momentum, and it is one of the transport phenomena originating from triangle anomaly. In Refs. [6,42], σ_χ has been computed in weak and strong coupling regimes in the limit $\vec{k} \rightarrow 0$ while k^0 is kept finite. Our formula shows that $A_{\pm\gamma}$ measures the imaginary part of the chiral magnetic conductivity in the kinematic domain of $k^0 = |\vec{k}|$ which hasn't been computed in literature before.

B. Dileptons

Let us continue our idea of identifying P- and CP-odd observables in the preceding subsection to the dilepton emissions from an isotropic axially charged QCD plasma.

We first derive that it is impossible to have P- and CP-odd observables in the dilepton emission rates if the lepton is strictly massless. Let us recall how P and C transformations act on the leptons and antileptons arising from quantizing a single massless Dirac field of the lepton species. For notational familiarity, we will denote leptons as e^- and antileptons e^+ . A single massless Dirac field divides into a left-handed Weyl field ψ_L and a right-handed Weyl field ψ_R . Upon quantization, ψ_L produces left-handed leptons e_L^- and right-handed antileptons e_R^+ , while ψ_R field produces right-handed leptons e_R^- and left-handed antileptons e_L^+ . The P transformation interchanges handedness without affecting the charges (that is \pm), and the C transformation interchanges the charges without affecting handedness,

$$\begin{aligned} P: e_L^- &\leftrightarrow e_R^-, & e_R^+ &\leftrightarrow e_L^+ \\ C: e_L^- &\leftrightarrow e_L^+, & e_R^- &\leftrightarrow e_R^+ \end{aligned} \quad (2.14)$$

The crucial point in the argument is that a dilepton pair is created from a virtual photon whose interaction vertex with the lepton field does not mix ψ_L and ψ_R , that is, the interaction Hamiltonian takes a form

$$H_I = ie \int d^3x A_\mu (\bar{\psi}_L \gamma^\mu \psi_L + \bar{\psi}_R \gamma^\mu \psi_R). \quad (2.15)$$

This implies that a created dilepton pair is either (e_L^-, e_R^+) or (e_R^-, e_L^+) , and other combinations are forbidden. Now imagine acting P and C transformations on the created dilepton pair. From (2.14), we have

$$\begin{aligned} P: (e_L^-, e_R^+) &\leftrightarrow (e_R^-, e_L^+) \\ C: (e_L^-, e_R^+) &\leftrightarrow (e_L^+, e_R^-) \end{aligned} \quad (2.16)$$

which shows that P and C transformations on our restricted set of allowed dilepton pairs are identical to each other. It is straightforward to conclude that it is impossible to have something which is P- and CP-odd (which requires to have C-even while P-odd). In our argument, we assumed that the interchange of the momenta of the final lepton and antilepton pair has no effect in the emission rate, which is true in an isotropic plasma when the magnitudes of the two momenta are the same and the rate depends only on the relative angle of the two momenta. More sophisticated situations with different magnitudes of momenta of the lepton and antilepton might allow some P- and CP-odd observables, but we have not explored this possibility, leaving it as an open question.

The above discussion brings us to consider a massive lepton species. We emphasize that this applies to all known leptons in nature including electrons, but we will see that our proposal for P- and CP-odd observable in dilepton emission rates is in fact proportional to the mass square of the lepton species, so that it vanishes for a massless species in line with the above discussion. This implies that the signal we propose should be more prominent for heavier lepton species.

Let us define our P- and CP-odd observable in dilepton emission rates. We focus on the case where the two momenta of the lepton and antilepton have the same magnitude, and form an angle 2θ . Calling the two momenta \vec{p}_1 and \vec{p}_2 , respectively, we conveniently choose them to be

$$\begin{aligned} \vec{p}_1 &= p(-\sin\theta, 0, \cos\theta), & \vec{p}_2 &= p(\sin\theta, 0, \cos\theta), \\ p &= |\vec{p}_1| = |\vec{p}_2|, \end{aligned} \quad (2.17)$$

which is schematically depicted in Fig. 1. The total center of mass four-momentum that is carried by the virtual photon is then

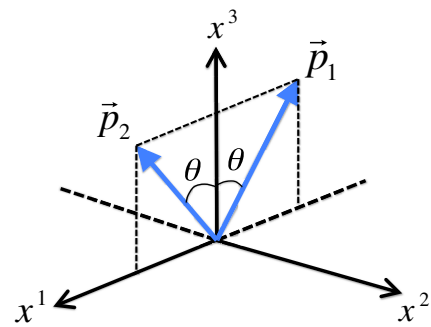


FIG. 1 (color online). A schematic illustration of the lepton (\vec{p}_1) and antilepton (\vec{p}_2) momenta in the dilepton emission from an isotropic axially charged plasma.

$$p_f^\mu = (2E, 0, 0, 2p \cos \theta), \quad E = \sqrt{p^2 + m^2}, \quad (2.18)$$

where m is the mass of the lepton species. The emitted lepton and antilepton carry $1/2$ spin degrees of freedom. For our purpose of discussing parity transformation, it is convenient to choose the helicity basis such that the $+1/2$ state is defined to be a state whose spin along the direction of the momentum is $+1/2$, and similarly for $-1/2$ state. Each massive lepton and antilepton can have the two possible spin states, and under parity P transformation, the helicity changes its sign. Let us denote the emission rate per unit volume and per unit phase spaces of lepton and antilepton with the spin states given by s_1 and s_2 , respectively, by Γ^{s_1, s_2} ,

$$\Gamma^{s_1, s_2} \equiv \frac{d\Gamma^{s_1, s_2}}{d^3 p_1 d^3 p_2}, \quad (2.19)$$

and for a given pair of momentum (\vec{p}_1, \vec{p}_2) , there are four possible rates $\Gamma^{\pm\frac{1}{2}, \pm\frac{1}{2}}$. Because of the rotational symmetry of the plasma, the rates with a fixed spin polarization depend only on the relative angle 2θ of the two momenta (\vec{p}_1, \vec{p}_2) . Under charge conjugation C , the lepton transforms to the antilepton without changing helicity, so that the actions of P and C on the spin-polarized emission rates are given by

$$\begin{aligned} P: \Gamma^{+\frac{1}{2}, +\frac{1}{2}} &\leftrightarrow \Gamma^{-\frac{1}{2}, -\frac{1}{2}}, & \Gamma^{+\frac{1}{2}, -\frac{1}{2}} &\leftrightarrow \Gamma^{-\frac{1}{2}, +\frac{1}{2}} \\ C: \Gamma^{\pm\frac{1}{2}, \pm\frac{1}{2}} &\leftrightarrow \Gamma^{\pm\frac{1}{2}, \pm\frac{1}{2}}, & \Gamma^{+\frac{1}{2}, -\frac{1}{2}} &\leftrightarrow \Gamma^{-\frac{1}{2}, +\frac{1}{2}} \end{aligned} \quad (2.20)$$

We see that in the subsector of $(\Gamma^{+1/2, -1/2}, \Gamma^{-1/2, +1/2})$ (i.e. the opposite spin polarizations for lepton and antilepton), the P and C transformations are identical to each other, hence it is impossible to have P and CP -odd observable from that sector. It is however possible to construct a simple P - and CP -odd observable from $\Gamma^{\pm 1/2, \pm 1/2}$ sector which is

$$A_{\pm\bar{l}\bar{l}} \equiv -\frac{\Gamma^{+\frac{1}{2}, +\frac{1}{2}} - \Gamma^{-\frac{1}{2}, -\frac{1}{2}}}{\Gamma^{+\frac{1}{2}, +\frac{1}{2}} + \Gamma^{-\frac{1}{2}, -\frac{1}{2}}}. \quad (2.21)$$

Note that the total dilepton rate

$$\Gamma_{\bar{l}\bar{l}} = \Gamma^{+\frac{1}{2}, +\frac{1}{2}} + \Gamma^{+\frac{1}{2}, -\frac{1}{2}} + \Gamma^{-\frac{1}{2}, +\frac{1}{2}} + \Gamma^{-\frac{1}{2}, -\frac{1}{2}}, \quad (2.22)$$

is what used to be computed in literature, and does not depend on the choice of the spin basis.

Let us discuss in detail how $A_{\pm\bar{l}\bar{l}}$ probes the P - and CP -odd properties of the QCD plasma. In Appendix B, we give a mundane quantum mechanics derivation of the dilepton emission rate with a specified spin polarization (s_1, s_2) given by

$$\begin{aligned} \Gamma^{s_1, s_2} &= \frac{d\Gamma^{s_1, s_2}}{d^3 p_1 d^3 p_2} \\ &= \frac{e^2 e_l^2}{(2\pi)^6} \left(\frac{1}{p_f^2}\right)^2 \frac{1}{2E_{\vec{p}_1}} \frac{1}{2E_{\vec{p}_2}} G_{\mu\nu}^<(p_f)(-1) \\ &\quad \times [\bar{v}(\vec{p}_2, s_2) \gamma^\mu u(\vec{p}_1, s_1)] [\bar{u}(\vec{p}_1, s_1) \gamma^\nu v(\vec{p}_2, s_2)], \end{aligned} \quad (2.23)$$

where $E_{\vec{p}} = \sqrt{\vec{p}^2 + m^2}$, $p_f^\mu = p_1^\mu + p_2^\mu$, the Wightman function $G_{\mu\nu}^<$ is defined in (2.4) before, and u, v are Dirac spinors of lepton and antilepton, respectively. Our convention for the Dirac matrices is

$$\{\gamma^\mu, \gamma^\nu\} = 2\eta^{\mu\nu}, \quad \eta = (-1, +1, +1, +1), \quad (2.24)$$

so that γ^0 is anti-Hermitian while γ^i ($i = 1, 2, 3$) are Hermitian. We will use the following explicit representation of them

$$\begin{aligned} \gamma^0 &= \begin{pmatrix} 0 & i\mathbf{1}_{2 \times 2} \\ i\mathbf{1}_{2 \times 2} & 0 \end{pmatrix}, & \gamma^i &= \begin{pmatrix} 0 & i\sigma^i \\ -i\sigma^i & 0 \end{pmatrix}, \\ & & i &= 1, 2, 3, \end{aligned} \quad (2.25)$$

upon which the spin matrix corresponding to a spatial rotation of angle θ along an axis \hat{n} is given simply by

$$S(\hat{n}, \theta) = e^{i\theta \vec{s} \cdot \hat{n}}, \quad S^i \equiv \frac{1}{2} \begin{pmatrix} \sigma^i & 0 \\ 0 & \sigma^i \end{pmatrix}. \quad (2.26)$$

Recall that the above acts on the lepton wave functions, both positive and negative energy states. For the antileptons which are holes of the lepton wave functions with negative energy, the actual spin matrix is in fact a negative of the above. Note also that our definition for $\bar{\psi}$ is $\bar{\psi} \equiv -i\psi^\dagger \gamma^0$, and the Dirac equation is $(\gamma^\mu \partial_\mu - m)\psi = 0$. With the above conventions, the Dirac spinors are given by

$$\begin{aligned} u(\vec{p}, s) &= \begin{pmatrix} \sqrt{E - \vec{p} \cdot \vec{\sigma}} \xi^s \\ \sqrt{E + \vec{p} \cdot \vec{\sigma}} \xi^s \end{pmatrix}, \\ v(\vec{p}, s) &= \begin{pmatrix} \sqrt{E - \vec{p} \cdot \vec{\sigma}} \eta^s \\ -\sqrt{E + \vec{p} \cdot \vec{\sigma}} \eta^s \end{pmatrix}, \end{aligned} \quad (2.27)$$

where

$$\begin{aligned} (\vec{p} \cdot \vec{\sigma}) \xi^s &= (2s) |\vec{p}| \xi^s, & (\vec{p} \cdot \vec{\sigma}) \eta^s &= -(2s) |\vec{p}| \eta^s, \\ s &= \pm \frac{1}{2}. \end{aligned} \quad (2.28)$$

With our choice of the momenta \vec{p}_1 and \vec{p}_2 as in Fig. 1, the Dirac spinors are explicitly found to be

$$u(\vec{p}_1, +1/2) = \begin{pmatrix} +\sqrt{E-p} \cos(\theta/2) \\ -\sqrt{E-p} \sin(\theta/2) \\ +\sqrt{E+p} \cos(\theta/2) \\ -\sqrt{E+p} \sin(\theta/2) \end{pmatrix}, \quad u(\vec{p}_1, -1/2) = \begin{pmatrix} +\sqrt{E+p} \sin(\theta/2) \\ +\sqrt{E+p} \cos(\theta/2) \\ +\sqrt{E-p} \sin(\theta/2) \\ +\sqrt{E-p} \cos(\theta/2) \end{pmatrix}, \quad (2.29)$$

and

$$v(\vec{p}_2, +1/2) = \begin{pmatrix} -\sqrt{E+p} \sin(\theta/2) \\ +\sqrt{E+p} \cos(\theta/2) \\ +\sqrt{E-p} \sin(\theta/2) \\ -\sqrt{E-p} \cos(\theta/2) \end{pmatrix}, \quad v(\vec{p}_2, -1/2) = \begin{pmatrix} +\sqrt{E-p} \cos(\theta/2) \\ +\sqrt{E-p} \sin(\theta/2) \\ -\sqrt{E+p} \cos(\theta/2) \\ -\sqrt{E+p} \sin(\theta/2) \end{pmatrix}. \quad (2.30)$$

With the above expressions, let us then compute the spin-polarization contracted Wightman function that the emission rate (2.23) is proportional to

$$\begin{aligned} G^{s_1, s_2} &\equiv (-1)G_{\mu\nu}^<(p_f)[\bar{v}(\vec{p}_2, s_2)\gamma^\mu u(\vec{p}_1, s_1)][\bar{u}(\vec{p}_1, s_1)\gamma^\nu v(\vec{p}_2, s_2)] \\ &= \frac{2}{e^{\beta p_f^0} - 1} \text{Im}[G_{\mu\nu}^R(p_f)[\bar{v}(\vec{p}_2, s_2)\gamma^\mu u(\vec{p}_1, s_1)][\bar{u}(\vec{p}_1, s_1)\gamma^\nu v(\vec{p}_2, s_2)]], \end{aligned} \quad (2.31)$$

where the second line is obtained from the standard manipulation with Lehmann representation, using the fact that what multiplies to $G_{\mu\nu}^<$ from Dirac spinors is Hermitian with respect to $\mu\nu$ indices (see Sec. 2 in Ref. [37]). After some algebra, we find

$$\begin{aligned} G^{\pm\frac{1}{2}, \pm\frac{1}{2}} &= 4m^2((1 + \cos^2\theta)G_{11}^< \mp 2i \cos\theta G_{12}^<) \\ &= 2m^2((1 \mp \cos\theta)^2(G_{11}^< + iG_{12}^<) + (1 \pm \cos\theta)^2(G_{11}^< - iG_{12}^<)) \\ &= \frac{-4m^2}{e^{\beta p_f^0} - 1} ((1 \mp \cos\theta)^2 \text{Im}(G_{11}^R + iG_{12}^R) + (1 \pm \cos\theta)^2 \text{Im}(G_{11}^R - iG_{12}^R)) \\ &= \frac{-4m^2}{e^{\beta p_f^0} - 1} ((1 \mp \cos\theta)^2 \text{Im}G_+^R + (1 \pm \cos\theta)^2 \text{Im}G_-^R), \end{aligned} \quad (2.32)$$

where we have used $G_{11}^R = G_{22}^R$ and $G_{12}^R = -G_{21}^R$ from the rotational symmetry as in (2.9), and $G_{\pm}^R \equiv (G_{11}^R \pm iG_{12}^R)$ as defined before. It is possible to compute $G^{\pm 1/2, \mp 1/2}$ too, but the results are not of interest to us. They are given by

$$\begin{aligned} G^{+\frac{1}{2}, -\frac{1}{2}} &= G^{-\frac{1}{2}, +\frac{1}{2}} \\ &= 4(p^2 \cos^2\theta - E^2)(G_{00}^< - G_{33}^<) + 4E^2 \sin^2\theta G_{11}^<, \end{aligned} \quad (2.33)$$

after using the Ward identity

$$EG_{00}^< + p \cos\theta G_{30}^< = 0, \quad EG_{03}^< + p \cos\theta G_{33}^< = 0. \quad (2.34)$$

We confirm that $G^{\pm 1/2, \pm 1/2}$ are proportional to the mass square of the lepton species, so that our P- and CP-odd observable $A_{\pm\bar{l}}$ constructed from them is well defined for a massive species only.

Using the above results, our final expression for P- and CP-odd observable $A_{\pm\bar{l}}$ in the dilepton emission rate in terms of retarded correlation functions is

$$A_{\pm\bar{l}} = \left(\frac{2 \cos\theta}{1 + \cos^2\theta} \right) \cdot \frac{\text{Im}G_+^R - \text{Im}G_-^R}{\text{Im}G_+^R + \text{Im}G_-^R} \Bigg|_{p^\mu = p_j^\mu = p_1^\mu + p_2^\mu}, \quad (2.35)$$

which is similar to the expression (2.12) for $A_{\pm\gamma}$, except an additional angular factor and a different kinematic domain

probed. We see that $A_{\pm\bar{l}}$ is also a consequence of the underlying triangle anomaly, and it measures the chiral magnetic conductivity in a different kinematic domain.

In the next section, we give an exemplar computation of ImG_{\pm}^R in strongly coupled regime, using AdS/CFT correspondence, and present some numerical results for our P- and CP-odd observables $A_{\pm\gamma}$ and $A_{\pm\bar{l}}$ that may be relevant in realistic heavy-ion experiments.

III. STRONG COUPLING COMPUTATION

The purpose of this section is to present one exemplar model computation of our P- and CP-odd observables $A_{\pm\gamma}$ and $A_{\pm\bar{l}}$ in strongly coupled regime using AdS/CFT correspondence. Since the chiral symmetry, especially the triangle anomaly represented by 5 dimensional Chern-Simons terms, is an important ingredient in our observables, the holographic model to be used should describe the right chiral symmetry in the real QCD. Instead of using a bottom-up approach, we choose to work in the Sakai-Sugimoto model [43] which is the only top-down holographic model whose chiral symmetry is identical to the one in QCD⁴.

For our purposes, it is enough to start from the following description of the model in its finite temperature deconfined phase. Our presentation is oriented only for its practical usage skipping details of its derivations (For a more complete description, see for example Sec. 5 of Ref. [42] and Sec. 3 of Ref. [37].) We consider the case of having a single massless Dirac quark species whose electric charge is e . The model lives in a 5 dimensional space-time, (x^μ, U) where U is an extra holographic dimension. There are two 5 dimensional U(1) gauge fields, A_V and A_a , corresponding to the vector and axial symmetry of the massless quark species in the QCD side, whose 5 dimensional dynamics describes the chiral dynamics of the massless quark holographically. Especially, there are 5 dimensional Chern-Simons terms that are the holographic manifestation of the triangle anomaly in the QCD side

$$S_{CS} = \frac{N_c}{96\pi^2} \int d^4x dU \epsilon^{MNPQR} [-(A_L)_M (F_L)_{NP} (F_L)_{QR} + (A_R)_M (F_R)_{NP} (F_R)_{QR}], \quad (3.1)$$

where we introduce chiral gauge fields defined by

$$A_L = A_V - A_a, \quad A_R = A_V + A_a. \quad (3.2)$$

⁴We should bear in mind that the background holographic space-time from the D4 branes in the deconfined phase of the model has a problem with center symmetry, which prevents us from relating it to the true gluonic sector of the real QCD [44]. However, this problem is absent for the chiral symmetry dynamics described by the probe D8 branes that our analysis is focused on.

The QCD plasma with a finite axial charge is described in the model by a nonzero background configuration of the axial gauge field A_a which is⁵

$$(F_a)_{iU}^{(0)} = -\frac{\alpha}{\sqrt{U^5 + \alpha^2}}, \quad (3.3)$$

where the parameter α is related to the axial chemical potential μ_A by the relation

$$\mu_A = \int_{U_T}^{\infty} dU \frac{\alpha}{\sqrt{U^5 + \alpha^2}} = \frac{2\alpha}{3U_T^{\frac{3}{2}}} {}_2F_1\left(\frac{3}{10}, \frac{1}{2}, \frac{13}{10}, -\frac{\alpha^2}{U_T^5}\right). \quad (3.4)$$

The parameter U_T in the above in turn is determined by the temperature T by

$$U_T = R^3 \left(\frac{4\pi T}{3}\right)^2, \quad (3.5)$$

with a numerical value $R^3 = 1.44$ in units of GeV. The U_T is in fact the location of the black-hole horizon at $U = U_T$ in the background holographic space-time describing a finite temperature plasma, and the holographic coordinate U has a range $U_T < U < \infty$ where $U = \infty$ is the region corresponding to the UV regime of the QCD side.

Our main interest is to compute retarded (vector) current correlation functions in the axially charged plasma described above. To do this in holography, one first solves the linearized equations of motion for the vector gauge field A_V fluctuations from the background solution given by (3.3) [42]

$$\begin{aligned} \partial_U(A(U)F_{iU}) - B(U)(\partial_i F_{Ui}) &= 0, \\ A(U)(\partial_i F_{iU}) + B(U)(\partial_i F_{ii}) + C(U)(\partial_i F_{Ui}) &= 0, \\ B(U)(\partial_i F_{Ui}) + \partial_U(B(U)F_{ii} + C(U)F_{Ui}) \\ + D(U)\partial_j F_{ji} - \frac{N_c}{8\pi^2 C} (F_a)_{iU}^{(0)} \epsilon^{ijk} F_{jk} &= 0, \end{aligned} \quad (3.6)$$

where $i, j, k = 1, 2, 3$, $C = 0.0211$ in units of GeV, and the functions $A(U)$, $B(U)$, $C(U)$, $D(U)$ are given by

$$\begin{aligned} A(U) &= U^{-5}(U^5 + \alpha^2)^{\frac{3}{2}}, \\ B(U) &= \left(\frac{R}{U}\right)^{\frac{3}{2}}(U^5 + \alpha^2)^{\frac{1}{2}}, \\ C(U) &= f(U)(U^5 + \alpha^2)^{\frac{1}{2}}, \\ D(U) &= \left(\frac{R}{U}\right)^3 U^5 (U^5 + \alpha^2)^{-\frac{1}{2}}, \end{aligned} \quad (3.7)$$

⁵We put $2\pi l_s^2 = 1$ in the formulas from Ref. [42] for convenience, since its value does not appear in the final QCD observables.

with

$$f(U) = 1 - \left(\frac{U_T}{U}\right)^3. \quad (3.8)$$

Note that the last term in the third equation in (3.6) is from the 5 dimensional Chern-Simons term which is a consequence of triangle anomaly. The solution has a near $U \rightarrow \infty$ behavior given by

$$A_\mu = A_\mu^{(0)} + \frac{A_\mu^{(1)}}{U^{\frac{1}{2}}} + \frac{A_\mu^{(2)}}{U} + \frac{\tilde{A}_\mu}{U^{\frac{3}{2}}} + \dots, \quad (3.9)$$

with

$$\begin{aligned} A_t^{(1)} &= 0, & A_t^{(2)} &= 2R^3 F_{tt}^{(0)}, \\ A_i^{(2)} &= -2R^3 \partial_j F_{ij}^{(0)}, & A_i^{(1)} &= -2R^3 \partial_j F_{ij}^{(0)}, \end{aligned} \quad (3.10)$$

where $A_\mu^{(0)}$ is a free parameter (the UV boundary condition) acting as a source for the QCD vector current J^μ , while the \tilde{A}_μ is a dynamically determined quantity which encodes the expectation value of the current in the presence of the source $A_\mu^{(0)}$ by [37]

$$\begin{aligned} \langle J_t \rangle &= 3C \left(\tilde{A}_t + \frac{8}{3} R^3 \partial_t \partial_j F_{ij}^{(0)} \right), \\ \langle J_i \rangle &= 3C \left(\tilde{A}_i + 4R^3 \left(\partial_t \partial_j F_{ij}^{(0)} + \frac{2}{3} \partial_t^2 F_{ii}^{(0)} - \frac{1}{3} \partial_i \partial_j F_{ij}^{(0)} \right) \right). \end{aligned} \quad (3.11)$$

The solution with a given source $A_\mu^{(0)}$ and the incoming boundary condition at the horizon $U = U_T$ is unique and it is proportional to $A_\mu^{(0)}$, and hence the current expectation value (3.11) is a linear function of $A_\mu^{(0)}$ from which we finally obtain our desired retarded correlation functions as

$$\langle J_\mu \rangle = -G_\mu^\nu A_\nu^{(0)}. \quad (3.12)$$

Since we are interested in computing only the transverse part of the correlation functions, we can consistently turn on $A_{1,2}$ components only, after taking the frequency-momentum $(\omega, \vec{k} = k\hat{x}^3)$, so that $\partial_t = -i\omega$, $\partial_i = ik\delta_{i3}$. The relevant equation of motion is the third equation in (3.6),

$$\begin{aligned} -i\omega B(U) \partial_U A_i + \partial_U (-i\omega B(U) A_i + C(U) \partial_U A_i) \\ - k^2 D(U) A_i + ik \frac{N_c}{8\pi^2 C} (F_a)_{iU}^{(0)} \epsilon^{ij} A_j = 0, \end{aligned} \quad (3.13)$$

with $i, j = 1, 2$ and $\epsilon^{12} = -\epsilon^{21} = +1$. From the structure of the above equation, it is natural to work with a helicity basis

$$A_\pm = \frac{1}{\sqrt{2}} (A_1 \mp iA_2), \quad (3.14)$$

in terms of which the equation of motion diagonalizes as

$$\begin{aligned} -i\omega B(U) \partial_U A_\pm + \partial_U (-i\omega B(U) A_\pm + C(U) \partial_U A_\pm) \\ - k^2 D(U) A_\pm \mp ik \frac{N_c}{8\pi^2 C} (F_a)_{iU}^{(0)} A_\pm = 0. \end{aligned} \quad (3.15)$$

Once we find the solution of A_\pm , we can read off the source $A_\pm^{(0)} = 1/\sqrt{2}(A_1^{(0)} \mp A_2^{(0)})$ and the expectation value via (3.11)

$$\begin{aligned} \langle J^\pm \rangle &= \frac{1}{\sqrt{2}} (J^1 \mp iJ^2) \\ &= 3C \left(\tilde{A}_\pm + 4R^3 (-i\omega) \left(k^2 - \frac{2}{3} \omega^2 \right) A_\pm^{(0)} \right). \end{aligned} \quad (3.16)$$

From the relation $\langle J^i \rangle = -G^{Rij} A_j^{(0)}$, and the rotational symmetry $G_{11}^R = G_{22}^R$ and $G_{12}^R = -G_{21}^R$, it is straight forward to see that

$$\langle J^\pm \rangle = -(G_{11}^R \pm iG_{12}^R) A_\pm^{(0)} = -G_\pm^R A_\pm^{(0)}, \quad (3.17)$$

so that we can naturally obtain our desired G_\pm^R , entering our expressions (2.12) and (2.35) for $A_{\pm\gamma}$ and $A_{\pm\bar{l}}$, from the solutions of A_\pm .

Numerically, what we do is to solve Eq. (3.15) from the horizon $U = U_T$ up to a UV maximum U_{\max} and then compare its value and derivative at U_{\max} with the UV expansion (3.9),

$$\begin{aligned} A_\pm(U_{\max}) &= A_\pm^{(0)} + \frac{2R^3(-i\omega)}{U_{\max}^{\frac{1}{2}}} A_\pm^{(0)} + \frac{-2R^3 k^2}{U_{\max}} A_\pm^{(0)} + \frac{\tilde{A}_\pm}{U_{\max}^{\frac{3}{2}}}, \\ \partial_U A_\pm(U_{\max}) &= -\frac{12R^3(-i\omega)}{2 U_{\max}^{\frac{3}{2}}} A_\pm^{(0)} + \frac{2R^3 k^2}{U_{\max}^2} A_\pm^{(0)} - \frac{3}{2} \frac{\tilde{A}_\pm}{U_{\max}^{\frac{5}{2}}}, \end{aligned} \quad (3.18)$$

to obtain $A_\pm^{(0)}$ and \tilde{A}_\pm . We then compute $\langle J^\pm \rangle$ from (3.16), and finally get G_\pm^R from

$$G_\pm^R = -\frac{\langle J^\pm \rangle}{A_\pm^{(0)}}. \quad (3.19)$$

Figure 2 shows our numerical results of photon circular polarization asymmetry $A_{\pm\gamma}$ as a function of frequency, where $T = 300$ MeV with $\mu_A = 100$ MeV (solid) and $\mu_A = 50$ MeV (dashed). Since the model is trustable only up to a few GeV's, we compute $A_{\pm\gamma}$ only for $\omega < 2$ GeV. We observe that the asymmetry is about a percent level with a peak around $\omega = 1$ GeV. It is easy to check that the result

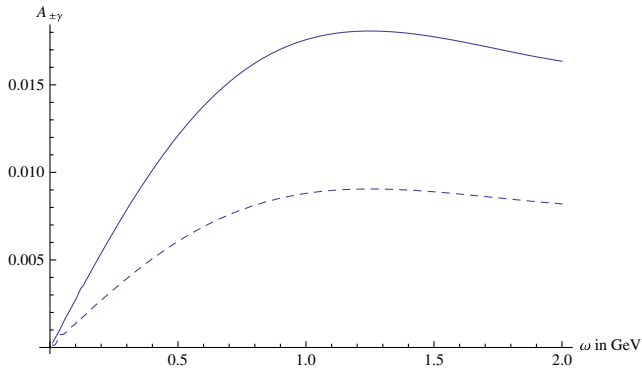


FIG. 2 (color online). The photon circular polarization asymmetry $A_{\pm\gamma}$ from an axially charged plasma as a function of frequency ω , where $T = 300$ MeV with $\mu_A = 100$ MeV (solid) and $\mu_A = 50$ MeV (dashed).

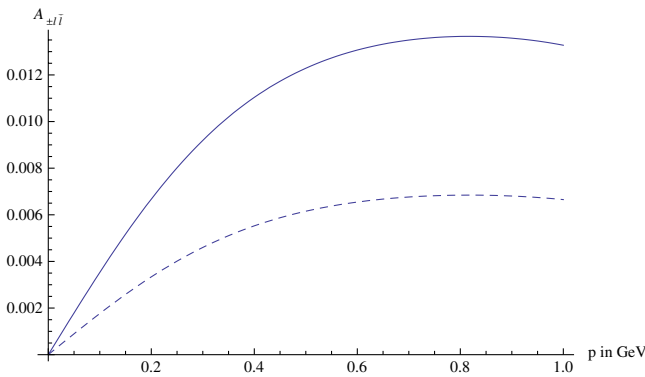


FIG. 3 (color online). The dilepton spin polarization asymmetry $A_{\pm\ell}$ from an axially charged plasma as a function of one lepton momentum $p = |\vec{p}|$ for the case of muon, where $T = 300$ MeV with $\mu_A = 100$ MeV (solid) and $\mu_A = 50$ MeV (dashed). The relative angle between muon and antimuon pair is taken to be $2\theta = \frac{\pi}{2}$.

is absent without the Chern-Simons term (triangle anomaly) and the effect is roughly proportional to the axial chemical potential.

Figure 3 shows our numerical results for the dilepton spin polarization asymmetry $A_{\pm\ell}$ in the case of a dimuon pair with a relative angle $2\theta = \frac{\pi}{2}$ as a function of the muon momentum $p = |\vec{p}|$ (see Fig. 1). Note that the p_f^μ which probes the plasma is

$$p_f^0 = 2\sqrt{p^2 + m_\mu^2}, \quad m_\mu = 100 \text{ MeV},$$

$$|\vec{p}_f| = 2p \cos \theta. \quad (3.20)$$

We observe again that the effect is about a percent level.

IV. DISCUSSION

In this work, we identify P- and CP-odd observables in the photons and dilepton emission rates from an axially

charged isotropic QCD plasma, whose experimental observation can be a direct confirmation of the triangle anomaly in QCD. Although at present, experimentally measuring polarization of photons and dileptons seems hard with the current detectors, it may be an interesting future direction to pursue. One possible channel is the spin dependent weak muon and antimuon decays since the weak interaction is chiral: only muons with left-handed spin (the “-” spin in our notation) would decay to $e^- + \bar{\nu}_e + \nu_\mu$ and only antimuons with right-handed spin (“+” spin) decay into $e^+ + \nu_e + \bar{\nu}_\mu$, so that a positive $A_{\pm\ell}$ would result in an excess of $e^+ + \nu_e + \bar{\nu}_\mu$ production compared to $e^- + \bar{\nu}_e + \nu_\mu$.

We show that these observables are proportional to the imaginary part of the chiral magnetic conductivity at a finite frequency-momentum region, which is originating from the underlying triangle anomaly. With an ideal set of parameters of the temperature and the axial chemical potential, our exemplar model computation in AdS/CFT correspondence shows that our observables are of a percent level. Clearly, a more realistic estimate of the net effect is desirable, including various real time fireball dynamics and the axial charge fluctuation dynamics in both early glasma phase and the later quark-gluon plasma stage. Another direction is to compute our observables in different models such as weak coupling chiral kinetic theory that has been recently developed in Refs. [45–47].

ACKNOWLEDGMENTS

We thank Adam Bzdak, Dima Kharzeev, Shu Lin, Larry McLerran, Vlad Skokov, Misha Stephanov, and Raju Venugopalan for interesting discussions.

APPENDIX A: PHOTON EMISSION FORMULA FROM QUANTUM MECHANICS

We derive the photon emission rate formula (2.3) in terms of the Wightman function $G_{\mu\nu}^<$,

$$\frac{d\Gamma}{d^3\vec{k}}(\epsilon^\mu) = \frac{e^2}{(2\pi)^3 2|\vec{k}|} \epsilon^\mu (\epsilon^\nu)^* G_{\mu\nu}^<(k) \Big|_{k^0=|\vec{k}|}, \quad (A1)$$

in the framework of quantum mechanics perturbation theory. The Hilbert space of our interest is a tensor product of the QCD plasma Hilbert space and the Hilbert space of photons,

$$\mathcal{H} = \mathcal{H}_{\text{QCD}} \otimes \mathcal{H}_\gamma. \quad (A2)$$

The photon emission process from a QCD plasma is a quantum mechanical transition from an initial state

$$|i\rangle = |\alpha_i\rangle \otimes |0\rangle, \quad (A3)$$

to a final state containing one photon quantum with a momentum \vec{k} and a polarization ϵ^μ ,

$$|f\rangle = |\alpha_f\rangle \otimes |\vec{k}, \epsilon^\mu\rangle, \quad (\text{A4})$$

where $|\alpha_{i,f}\rangle$ are QCD states describing the plasma. We will perform a thermal ensemble average for the initial QCD state $|\alpha_i\rangle$, while summing over all possible final QCD states $|\alpha_f\rangle$ to get a final emission rate for a fixed photon state $|\vec{k}, \epsilon^\mu\rangle$.

The transition from our initial state to the final state with one photon arises due to an interaction Hamiltonian

$$H_I = e \int d^3x A_\mu(\vec{x}, t=0) J^\mu(\vec{x}, t=0), \quad (\text{A5})$$

where A_μ is the photon field operator and J^μ is the electromagnetic current operator in the QCD sector. Note that A_μ acts only on \mathcal{H}_γ , and J^μ on \mathcal{H}_{QCD} only. Since it is easy to see that the matrix element of H_I between our initial and final states is nonzero, the transition process is described by a first order perturbation theory where the transition rate is given by Fermi's golden rule

$$T_{i \rightarrow f} = (2\pi) |\langle f | H_I | i \rangle|^2 \delta(E_f - E_i), \quad (\text{A6})$$

where $E_{i,f}$ are the energies of the initial and final states. In this expression, it is important to have the right normalization for the states, $\langle i | i \rangle = \langle f | f \rangle = 1$. To keep track of normalization of the states properly, we work in a finite volume case throughout our derivation until we take an infinite volume limit at the end. A spatial momentum in a finite volume V is discrete and labeled by a triple of integers \vec{n} , so that we denote it as $\vec{k}_{\vec{n}}$. The number of such momentum states in a phase space volume d^3k is well known to be $V \frac{d^3k}{(2\pi)^3}$.

The photon field operator $A_\mu(\vec{x}, t)$ in a finite volume V has a standard expansion in terms of creation and annihilation operators of individual photon states with momenta $\vec{k}_{\vec{n}}$ and polarization $\epsilon_\mu^{(s)}$ as

$$A_\mu(\vec{x}, t) = \frac{1}{V} \sum_{\vec{n}, s} \frac{1}{\sqrt{2|\vec{k}_{\vec{n}}|}} (\epsilon_\mu^{(s)} a_{\vec{k}_{\vec{n}}}^{(s)} e^{-i|\vec{k}_{\vec{n}}|t + i\vec{k}_{\vec{n}} \cdot \vec{x}} + h.c.), \quad (\text{A7})$$

where the creation/annihilation operators satisfy

$$\left[a_{\vec{k}_{\vec{n}}}^{(s)}, a_{\vec{k}_{\vec{n}'}}^{(s')\dagger} \right] = V \delta_{\vec{n}, \vec{n}'} \delta^{s, s'}. \quad (\text{A8})$$

In the above, we are careful about how the volume factors enter to have a right normalization of the field commutation relations. With this, the properly normalized one photon state in the Hilbert space \mathcal{H}_γ is

$$|\vec{k}_{\vec{n}}, s\rangle = \frac{1}{\sqrt{V}} a_{\vec{k}_{\vec{n}}}^{(s)\dagger} |0\rangle. \quad (\text{A9})$$

It is then straightforward to compute the matrix element $\langle f | H_I | i \rangle$ for our initial and final states (A3) and (A4). Using

$$\langle \vec{k}_{\vec{n}}, s | A_\mu(\vec{x}, t=0) | 0 \rangle = \frac{1}{\sqrt{V}} \frac{1}{\sqrt{2|\vec{k}_{\vec{n}}|}} \epsilon_\mu^{(s)*} e^{-i\vec{k}_{\vec{n}} \cdot \vec{x}}, \quad (\text{A10})$$

we have

$$\begin{aligned} \langle f | H_I | i \rangle &= \frac{1}{\sqrt{V}} \frac{e}{\sqrt{2|\vec{k}_{\vec{n}}|}} \epsilon_\mu^{(s)*} \\ &\times \int d^3x \langle \alpha_f | J^\mu(\vec{x}, t=0) | \alpha_i \rangle e^{-i\vec{k}_{\vec{n}} \cdot \vec{x}}. \end{aligned} \quad (\text{A11})$$

Denoting the energies of the QCD states $|\alpha_{i,f}\rangle$ by $\epsilon_{i,f}$, the initial and final state energies are $E_i = \epsilon_i$ and $E_f = \epsilon_f + |\vec{k}_{\vec{n}}|$, so that the transition rate by (A6) becomes

$$\begin{aligned} T_{i \rightarrow f} &= \frac{(2\pi)}{V} \frac{e^2}{2|\vec{k}_{\vec{n}}|} \epsilon_\mu^{(s)*} \epsilon_\nu^{(s)} \delta(\epsilon_f - \epsilon_i + |\vec{k}_{\vec{n}}|) \\ &\times \int d^3x \int d^3y e^{i\vec{k}_{\vec{n}} \cdot (\vec{y} - \vec{x})} \langle \alpha_i | J^\nu(\vec{y}, t=0) | \alpha_f \rangle \\ &\times \langle \alpha_f | J^\mu(\vec{x}, t=0) | \alpha_i \rangle. \end{aligned} \quad (\text{A12})$$

We now do the following manipulation on the above. We first replace $\delta(\epsilon_f - \epsilon_i + |\vec{k}_{\vec{n}}|)$ by

$$\delta(\epsilon_f - \epsilon_i + |\vec{k}_{\vec{n}}|) = \frac{1}{2\pi} \int dt e^{it(\epsilon_f - \epsilon_i + |\vec{k}_{\vec{n}}|)}, \quad (\text{A13})$$

and combine the factor $e^{it(\epsilon_f - \epsilon_i)}$ from the above with $\langle \alpha_f | J^\mu(\vec{x}, t=0) | \alpha_i \rangle$ to have

$$e^{it(\epsilon_f - \epsilon_i)} \langle \alpha_f | J^\mu(\vec{x}, t=0) | \alpha_i \rangle = \langle \alpha_f | J^\mu(\vec{x}, t) | \alpha_i \rangle, \quad (\text{A14})$$

using the fact that $J^\mu(\vec{x}, t) = e^{iHt} J^\mu(\vec{x}, t=0) e^{-iHt}$. The result is

$$\begin{aligned} T_{i \rightarrow f} &= \frac{1}{V} \frac{e^2}{2|\vec{k}_{\vec{n}}|} \epsilon_\mu^{(s)*} \epsilon_\nu^{(s)} \int d^3x \int d^3y \\ &\times \int dt e^{i|\vec{k}_{\vec{n}}|t + i\vec{k}_{\vec{n}} \cdot (\vec{y} - \vec{x})} \langle \alpha_i | J^\nu(\vec{y}, t=0) | \alpha_f \rangle \\ &\times \langle \alpha_f | J^\mu(\vec{x}, t) | \alpha_i \rangle. \end{aligned} \quad (\text{A15})$$

We then sum over the final QCD states $|\alpha_f\rangle$ to remove $\sum_f |\alpha_f\rangle \langle \alpha_f| = 1$ in the middle, and perform a thermal ensemble average over α_i ,

$$\begin{aligned} & \langle J^\nu(\vec{y}, t=0) J^\mu(\vec{x}, t) \rangle \\ & \equiv \frac{1}{Z} \sum_i e^{-\beta \epsilon_i} \langle \alpha_i | J^\nu(\vec{y}, t=0) J^\mu(\vec{x}, t) | \alpha_i \rangle, \end{aligned} \quad (\text{A16})$$

to have

$$\begin{aligned} T_{i \rightarrow f} &= \frac{1}{V} \frac{e^2}{2|\vec{k}_{\vec{n}}|} \epsilon_\mu^{(s)*} \epsilon_\nu^{(s)} \int d^3x \int d^3y \\ & \times \int dt e^{i|\vec{k}_{\vec{n}}|t + i\vec{k}_{\vec{n}} \cdot (\vec{y} - \vec{x})} \langle J^\nu(\vec{y}, t=0) J^\mu(\vec{x}, t) \rangle. \end{aligned} \quad (\text{A17})$$

Exploring the translational symmetry of the plasma such that $\langle J^\nu(\vec{y}, t=0) J^\mu(\vec{x}, t) \rangle$ depends only on the relative displacement $\vec{x} - \vec{y}$, one can simply replace $\vec{x} - \vec{y}$ with \vec{x} in the integrand while getting additional volume factor $\int d^3y = V$, to have

$$\begin{aligned} T_{i \rightarrow f} &= \frac{e^2}{2|\vec{k}_{\vec{n}}|} \epsilon_\mu^{(s)*} \epsilon_\nu^{(s)} \int d^3x \\ & \times \int dt e^{i|\vec{k}_{\vec{n}}|t - i\vec{k}_{\vec{n}} \cdot \vec{x}} \langle J^\nu(\vec{0}, t=0) J^\mu(\vec{x}, t) \rangle \\ & = \frac{e^2}{2|\vec{k}_{\vec{n}}|} \epsilon^{(s)\mu*} \epsilon^{(s)\nu} G_{\nu\mu}^<(k^0 = |\vec{k}_{\vec{n}}|, \vec{k}_{\vec{n}}), \end{aligned} \quad (\text{A18})$$

where the Wightman function is defined as before

$$G_{\nu\mu}^<(k) = \int d^4x e^{-ikx} \langle J_\mu(0) J_\nu(x) \rangle. \quad (\text{A19})$$

Recalling that the number of momentum states within a phase space volume d^3k is $V \frac{d^3k}{(2\pi)^3}$, the total transition rate to the states having one photon within a phase space volume d^3k is obtained by multiplying the above $T_{i \rightarrow f}$ by $V \frac{d^3k}{(2\pi)^3}$. Then, the photon emission rate per unit volume and per unit phase space volume is

$$\begin{aligned} \frac{d\Gamma}{d^3k} &= \frac{1}{(2\pi)^3} T_{i \rightarrow f} \\ &= \frac{e^2}{(2\pi)^3 2|\vec{k}_{\vec{n}}|} \epsilon^{(s)\mu*} \epsilon^{(s)\nu} G_{\nu\mu}^<(k^0 = |\vec{k}_{\vec{n}}|, \vec{k}_{\vec{n}}), \end{aligned} \quad (\text{A20})$$

which is our desired formula (A1) after taking an infinite volume limit to replace discrete $\vec{k}_{\vec{n}}$ with a continuum \vec{k} .

APPENDIX B: DILEPTON EMISSION FORMULA FROM QUANTUM MECHANICS

We would like to give a quantum mechanics derivation of the dilepton emission formula (2.23),

$$\begin{aligned} \frac{d\Gamma^{s_1, s_2}}{d^3p_1 d^3p_2} &= \frac{e^2 e_l^2}{(2\pi)^6} \left(\frac{1}{p_f^2} \right)^2 \frac{1}{2E_{\vec{p}_1}} \frac{1}{2E_{\vec{p}_2}} G_{\mu\nu}^<(p_f) \\ & \times (-1) [\bar{v}(\vec{p}_2, s_2) \gamma^\mu u(\vec{p}_1, s_1)] [\bar{u}(\vec{p}_1, s_1) \gamma^\nu v \\ & \times (\vec{p}_2, s_2)], \end{aligned} \quad (\text{B1})$$

where $p_f = p_1 + p_2$ is the total dilepton energy-momentum and e_l is the electric charge of the lepton species. The Hilbert space of our interests consists of three parts, the QCD sector \mathcal{H}_{QCD} , the photon sector \mathcal{H}_γ , and the lepton sector \mathcal{H}_l ; $\mathcal{H} = \mathcal{H}_{\text{QCD}} \otimes \mathcal{H}_\gamma \otimes \mathcal{H}_l$. The dilepton emission process is a transition from the initial state

$$|i\rangle = |\alpha_i\rangle \otimes |0\rangle \otimes |0\rangle, \quad (\text{B2})$$

to a final state containing the lepton and antilepton pair with momenta $\vec{p}_{1,2}$ and spin polarizations $s_{1,2}$, respectively,

$$|f\rangle = |\alpha_f\rangle \otimes |0\rangle \otimes |\vec{p}_1, s_1; \vec{p}_2, s_2\rangle. \quad (\text{B3})$$

The interaction Hamiltonian responsible for the transition is given by

$$\begin{aligned} H_I &= e \int d^3x A_\mu(\vec{x}, t=0) J^\mu(\vec{x}, t=0) + i e_l \\ & \times \int d^3x A_\mu(\vec{x}, t=0) \bar{\psi} \gamma^\mu \psi(\vec{x}, t=0), \end{aligned} \quad (\text{B4})$$

where ψ is the lepton field operator. Noting that J^μ acts on \mathcal{H}_{QCD} only, and similarly A_μ acts on \mathcal{H}_γ , and $\bar{\psi} \gamma^\mu \psi$ on \mathcal{H}_l , it is easy to see that the matrix element of H_I between our initial and final states (B2), (B3) vanishes

$$\langle f | H_I | i \rangle = 0, \quad (\text{B5})$$

so that there is no first order transition. This brings us to consider a second order perturbation theory where the initial state first makes a transition to an intermediate state $|m\rangle$ and the intermediate state makes a transition to our final state. Inspecting H_I , it is clear that the intermediate state $|m\rangle$ should contain one photon quantum to have a net non-vanishing transition by H_I . For the situation like ours where the transition is allowed only at the second order perturbation theory, we have to use the corresponding Fermi's golden rule at the second order perturbation theory,

$$T_{i \rightarrow f} = (2\pi) \left| \sum_m \frac{\langle f | H_I | m \rangle \langle m | H_I | i \rangle}{E_m - E_i} \right|^2 \delta(E_f - E_i). \quad (\text{B6})$$

From the structure of H_I , we find that there are two classes of possible intermediate states

Case A: The intermediate state involves one photon state only

$$|m\rangle = |\alpha_m\rangle \otimes |\vec{k}, \epsilon_\mu^{(s)}\rangle \otimes |0\rangle, \quad (\text{B7})$$

and this intermediate photon decays to the final dilepton pair.

Case B: The intermediate state consists of one photon and the dilepton pair,

$$|m\rangle = |\alpha_m\rangle \otimes |\vec{k}, \epsilon_\mu^{(s)}\rangle \otimes |\vec{p}_1, s_1; \vec{p}_2, s_2\rangle, \quad (\text{B8})$$

and the intermediate photon is subsequently absorbed by the QCD plasma to leave the dilepton pair in the final state.

Case A is more intuitive from the picture of the relativistic Feynman diagram of having a virtual photon line between the QCD current and the final dilepton pair. Case B in fact arises from the same Feynman diagram with a reversed time ordering where the QCD current operator appears later than the photon-lepton interaction vertex. Only after summing the two cases A and B in our mundane quantum mechanics treatment can we reproduce the relativistic result from a single Feynman diagram with a relativistic photon propagator. We will be able to check this shortly.

The quantization of the photon field A_μ in a finite volume V is explained in (A7) in the Appendix A, and we have a similar quantization of the lepton field ψ as

$$\begin{aligned} \psi(\vec{x}, t) = & \frac{1}{V} \sum_{\vec{n}, s} \frac{1}{\sqrt{2E_{\vec{p}_n}}} (u(\vec{p}_n, s) e^{-iE_{\vec{p}_n} t + i\vec{p}_n \cdot \vec{x}} a_{\vec{p}_n}^{(s)} \\ & + v(\vec{p}_n, s) e^{+iE_{\vec{p}_n} t - i\vec{p}_n \cdot \vec{x}} b_{\vec{p}_n}^{(s)\dagger}), \end{aligned} \quad (\text{B9})$$

where $(a_{\vec{p}_n}^{(s)}, b_{\vec{p}_n}^{(s)})$ are annihilation operators of lepton and antilepton, respectively, which satisfy the anticommutation relations

$$\{a_{\vec{p}_n}^{(s)}, a_{\vec{p}_n'}^{(s')\dagger}\} = \{b_{\vec{p}_n}^{(s)}, b_{\vec{p}_n'}^{(s')\dagger}\} = V \delta_{\vec{n}, \vec{n}'} \delta^{s, s'}. \quad (\text{B10})$$

Our conventions for the Dirac spinors u and v are explained in (2.27) in Sec. IIB. The properly normalized dilepton state in a finite volume is

$$|\vec{p}_{\vec{n}_1}, s_1; \vec{p}_{\vec{n}_2}, s_2\rangle = \frac{1}{V} a_{\vec{p}_{\vec{n}_1}}^{(s_1)\dagger} b_{\vec{p}_{\vec{n}_2}}^{(s_2)\dagger} |0\rangle. \quad (\text{B11})$$

We are now ready to compute the matrix elements of H_I .

Case A: Taking the intermediate state $|m\rangle = |\alpha_m\rangle \otimes |\vec{k}_n, \epsilon_\mu^{(s)}\rangle \otimes |0\rangle$, we have

$$\begin{aligned} \langle m|H_I|i\rangle = & \frac{1}{\sqrt{V}} \frac{e}{\sqrt{2|\vec{k}_n|}} \epsilon_\mu^{(s)*} \\ & \times \int d^3x e^{-i\vec{k}_n \cdot \vec{x}} \langle \alpha_m | J^\mu(\vec{x}, t=0) | \alpha_i \rangle, \end{aligned} \quad (\text{B12})$$

and after some algebra,

$$\begin{aligned} \langle f|H_I|m\rangle = & \frac{i}{\sqrt{V}} \frac{e_l}{\sqrt{2|\vec{k}_n|}} \frac{1}{\sqrt{2E_{\vec{p}_{\vec{n}_1}}}} \frac{1}{\sqrt{2E_{\vec{p}_{\vec{n}_2}}}} \epsilon_\nu^{(s)} \bar{u}(\vec{p}_{\vec{n}_1}, s_1) \gamma^\nu v \\ & \times (\vec{p}_{\vec{n}_2}, s_2) \delta_{\alpha_f, \alpha_m} \delta_{\vec{k}_n, -(\vec{p}_{\vec{n}_1} + \vec{p}_{\vec{n}_2})}. \end{aligned} \quad (\text{B13})$$

Since the energies of the states are $E_i = \epsilon_i$, $E_m = \epsilon_m + |\vec{k}_n|$, and $E_f = \epsilon_f + E_{\vec{p}_{\vec{n}_1}} + E_{\vec{p}_{\vec{n}_2}}$, we have

$$\begin{aligned} E_m - E_i = & \epsilon_m - \epsilon_i + |\vec{k}_n| = \epsilon_f - \epsilon_i + |\vec{k}_n| \\ = & -(E_{\vec{p}_{\vec{n}_1}} + E_{\vec{p}_{\vec{n}_2}}) + |\vec{p}_{\vec{n}_1} + \vec{p}_{\vec{n}_2}|, \end{aligned} \quad (\text{B14})$$

where we have used $\epsilon_m = \epsilon_f$ from $\delta_{\alpha_f, \alpha_m}$ in (B13), and the $\delta(E_f - E_i)$ factor in Fermi's golden rule gives us the equality

$$\epsilon_f - \epsilon_i = -(E_{\vec{p}_{\vec{n}_1}} + E_{\vec{p}_{\vec{n}_2}}), \quad (\text{B15})$$

and finally we replace \vec{k}_n with $\vec{p}_{\vec{n}_1} + \vec{p}_{\vec{n}_2}$ due to the $\delta_{\vec{k}_n, -(\vec{p}_{\vec{n}_1} + \vec{p}_{\vec{n}_2})}$ term in (B13). Note that the sum over the intermediate states reduces to a sum over the intermediate photon polarizations only, since $|\alpha_m\rangle = |\alpha_f\rangle$ and $\vec{k}_n = \vec{p}_{\vec{n}_1} + \vec{p}_{\vec{n}_2}$. Collecting things together, we have

$$\begin{aligned} & \sum_m \frac{\langle f|H_I|m\rangle \langle m|H_I|i\rangle}{E_m - E_i} \Big|_A \\ = & \frac{i}{V} \frac{e e_l}{(-p_f^0 + |\vec{p}_f|)} \frac{1}{2|\vec{p}_f|} \frac{1}{\sqrt{2E_{\vec{p}_{\vec{n}_1}}}} \frac{1}{\sqrt{2E_{\vec{p}_{\vec{n}_2}}}} \\ & \times \left(\sum_s \epsilon_\mu^{(s)*} \epsilon_\nu^{(s)} \right) \bar{u}(\vec{p}_{\vec{n}_1}, s_1) \gamma^\nu v(\vec{p}_{\vec{n}_2}, s_2) \\ & \times \int d^3x e^{-i\vec{p}_f \cdot \vec{x}} \langle \alpha_f | J^\mu(\vec{x}, t=0) | \alpha_i \rangle, \end{aligned} \quad (\text{B16})$$

where

$$p_f^\mu = (E_{\vec{p}_{\vec{n}_1}} + E_{\vec{p}_{\vec{n}_2}}, \vec{p}_{\vec{n}_1} + \vec{p}_{\vec{n}_2}), \quad (\text{B17})$$

is the total energy-momentum of the di-lepton pair.

Case B: With another class of the intermediate states $|m\rangle = |\alpha_m\rangle \otimes |\vec{k}_n, \epsilon_\mu^{(s)}\rangle \otimes |\vec{p}_{\vec{n}_1}, s_1; \vec{p}_{\vec{n}_2}, s_2\rangle$, a similar computation gives

$$\begin{aligned} \langle m|H_I|i\rangle = & \frac{i}{\sqrt{V}} \frac{e_l}{\sqrt{2|\vec{k}_n|}} \frac{1}{\sqrt{2E_{\vec{p}_{\vec{n}_1}}}} \frac{1}{\sqrt{2E_{\vec{p}_{\vec{n}_2}}}} \epsilon_\nu^{(s)*} \bar{u}(\vec{p}_{\vec{n}_1}, s_1) \gamma^\nu v \\ & \times (\vec{p}_{\vec{n}_2}, s_2) \delta_{\alpha_m, \alpha_i} \delta_{\vec{k}_n, -(\vec{p}_{\vec{n}_1} + \vec{p}_{\vec{n}_2})}, \end{aligned} \quad (\text{B18})$$

and

$$\langle f|H_I|m\rangle = \frac{1}{\sqrt{V}} \frac{e}{\sqrt{2|\vec{k}_{\vec{n}}|}} \epsilon_{\mu}^{(s)} \int d^3x e^{i\vec{k}_{\vec{n}}\cdot\vec{x}} \langle \alpha_f | J^{\mu}(\vec{x}, t=0) | \alpha_m \rangle, \quad (\text{B19})$$

and the summation over intermediate states reduces to a photon polarization sum as $|\alpha_m\rangle = |\alpha_i\rangle$ and $\vec{k}_{\vec{n}} = -(\vec{p}_{\vec{n}_1} + \vec{p}_{\vec{n}_2})$ due to the delta functions in (B18). The energies of the states are $E_i = \varepsilon_i$, $E_m = \varepsilon_m + |\vec{k}_{\vec{n}}| + E_{\vec{p}_{\vec{n}_1}} + E_{\vec{p}_{\vec{n}_2}} = \varepsilon_i + |\vec{p}_{\vec{f}}| + p_f^0$, and $E_f = \varepsilon_f + E_{\vec{p}_{\vec{n}_1}} + E_{\vec{p}_{\vec{n}_2}} = \varepsilon_f + p_f^0$, so that the energy denominator is

$$E_m - E_i = p_f^0 + |\vec{p}_{\vec{f}}|, \quad (\text{B20})$$

which gives us

$$\begin{aligned} & \sum_m \frac{\langle f|H_I|m\rangle \langle m|H_I|i\rangle}{E_m - E_i} \Big|_{\text{B}} \\ &= \frac{i}{V} \frac{ee_l}{(p_f^0 + |\vec{p}_{\vec{f}}|) 2|\vec{p}_{\vec{f}}|} \frac{1}{\sqrt{2E_{\vec{p}_{\vec{n}_1}}}} \frac{1}{\sqrt{2E_{\vec{p}_{\vec{n}_2}}}} \left(\sum_s \epsilon_{\mu}^{(s)} \epsilon_{\nu}^{(s)*} \right) \\ & \times \bar{u}(\vec{p}_{\vec{n}_1}, s_1) \gamma^{\nu} v(\vec{p}_{\vec{n}_2}, s_2) \int d^3x e^{-i\vec{p}_{\vec{f}}\cdot\vec{x}} \langle \alpha_f | J^{\mu}(\vec{x}, t=0) | \alpha_i \rangle, \end{aligned} \quad (\text{B21})$$

which is almost the same with (B16) except the energy denominator and the complex conjugation of the polarization sum.

The polarization sums, $\sum_s \epsilon_{\mu}^{(s)*} \epsilon_{\nu}^{(s)}$ and $\sum_s \epsilon_{\mu}^{(s)} \epsilon_{\nu}^{(s)*}$, should be replaced by a relativistic tensor,

$$\sum_s \epsilon_{\mu}^{(s)*} \epsilon_{\nu}^{(s)} = \sum_s \epsilon_{\mu}^{(s)} \epsilon_{\nu}^{(s)*} \rightarrow \eta_{\mu\nu}, \quad (\text{B22})$$

in a fully relativistic quantization of the gauge field, which can be justified for example in the Gupta-Bleuler quantization that involves unphysical ghost states in a subtle way. We will here simply take it as a working recipe.

After this replacement, (B16) and (B21) differ only by the energy denominator, and the addition of the two finally gives

$$\begin{aligned} & \sum_m \frac{\langle f|H_I|m\rangle \langle m|H_I|i\rangle}{E_m - E_i} \\ &= \frac{i}{V} \frac{ee_l}{p_f^2} \frac{1}{\sqrt{2E_{\vec{p}_{\vec{n}_1}}}} \frac{1}{\sqrt{2E_{\vec{p}_{\vec{n}_2}}}} \bar{u}(\vec{p}_{\vec{n}_1}, s_1) \gamma^{\mu} v(\vec{p}_{\vec{n}_2}, s_2) \\ & \times \int d^3x e^{-i\vec{p}_{\vec{f}}\cdot\vec{x}} \langle \alpha_f | J_{\mu}(\vec{x}, t=0) | \alpha_i \rangle, \end{aligned} \quad (\text{B23})$$

where $p_f^2 = -(p_f^0)^2 + |\vec{p}_{\vec{f}}|^2$ is precisely the relativistic denominator of the photon propagator in the Feynman diagram. Therefore, the sum of the two cases A and B reproduces the relativistic result.

Taking the square of (B23) and performing the same manipulations for $T_{i \rightarrow f}$ that we do for the case of the photon emission in the previous section noting that $E_f - E_i = \varepsilon_f - \varepsilon_i + p_f^0$, we arrive at

$$\begin{aligned} T_{i \rightarrow f} &= \frac{1}{V} \frac{e^2 e_l^2}{(p_f^2)^2} \frac{1}{2E_{\vec{p}_{\vec{n}_1}}} \frac{1}{2E_{\vec{p}_{\vec{n}_2}}} [\bar{u}(\vec{p}_{\vec{n}_1}, s_1) \gamma^{\mu} v(\vec{p}_{\vec{n}_2}, s_2)] \\ & \times [\bar{u}(\vec{p}_{\vec{n}_1}, s_1) \gamma^{\nu} v(\vec{p}_{\vec{n}_2}, s_2)]^* G_{\nu\mu}^<(p_f) \\ &= \frac{1}{V} \frac{e^2 e_l^2}{(p_f^2)^2} \frac{1}{2E_{\vec{p}_{\vec{n}_1}}} \frac{1}{2E_{\vec{p}_{\vec{n}_2}}} (-1) [\bar{u}(\vec{p}_{\vec{n}_1}, s_1) \gamma^{\mu} v(\vec{p}_{\vec{n}_2}, s_2)] \\ & \times [\bar{v}(\vec{p}_{\vec{n}_2}, s_2) \gamma^{\nu} u(\vec{p}_{\vec{n}_1}, s_1)] G_{\nu\mu}^<(p_f), \end{aligned} \quad (\text{B24})$$

using the fact that $[\bar{u}(\vec{p}_{\vec{n}_1}, s_1) \gamma^{\nu} v(\vec{p}_{\vec{n}_2}, s_2)]^* = -[\bar{v}(\vec{p}_{\vec{n}_2}, s_2) \gamma^{\nu} u(\vec{p}_{\vec{n}_1}, s_1)]$. The number of momentum pairs (\vec{p}_1, \vec{p}_2) within the phase space volume $d^3p_1 d^3p_2$ is $V^2 / (2\pi)^6 d^3p_1 d^3p_2$, so that the total transition rate into such states is the product of $T_{i \rightarrow f}$ and $V^2 / (2\pi)^6 d^3p_1 d^3p_2$, and therefore the transition rate per unit volume and per unit phase space $d^3p_1 d^3p_2$ for a pair of lepton and antilepton is finally given by

$$\begin{aligned} \frac{d\Gamma^{s_1, s_2}}{d^3p_1 d^3p_2} &= \frac{V}{(2\pi)^6} T_{i \rightarrow f} \\ &= \frac{1}{(2\pi)^6} \frac{e^2 e_l^2}{(p_f^2)^2} \frac{1}{2E_{\vec{p}_1}} \frac{1}{2E_{\vec{p}_2}} (-1) \\ & \times [\bar{u}(\vec{p}_1, s_1) \gamma^{\mu} v(\vec{p}_2, s_2)] [\bar{v}(\vec{p}_2, s_2) \gamma^{\nu} u \\ & \times (\vec{p}_1, s_1)] G_{\nu\mu}^<(p_f), \end{aligned} \quad (\text{B25})$$

after taking the infinite volume limit, which is our desired formula (B1).

- [1] D. Kharzeev and A. Zhitnitsky, *Nucl. Phys.* **A797**, 67 (2007).
- [2] D. E. Kharzeev, L. D. McLerran, and H. J. Warringa, *Nucl. Phys.* **A803**, 227 (2008).
- [3] K. Fukushima, D. E. Kharzeev, and H. J. Warringa, *Phys. Rev. D* **78**, 074033 (2008).
- [4] D. T. Son and A. R. Zhitnitsky, *Phys. Rev. D* **70**, 074018 (2004).
- [5] M. A. Metlitski and A. R. Zhitnitsky, *Phys. Rev. D* **72**, 045011 (2005).
- [6] D. E. Kharzeev and H. J. Warringa, *Phys. Rev. D* **80**, 034028 (2009).
- [7] D. Kharzeev, A. Krasnitz, and R. Venugopalan, *Phys. Lett. B* **545**, 298 (2002).
- [8] T. Lappi and L. McLerran, *Nucl. Phys.* **A772**, 200 (2006).
- [9] S. A. Voloshin, *Phys. Rev. C* **70**, 057901 (2004).
- [10] B. I. Abelev *et al.* (STAR Collaboration), *Phys. Rev. Lett.* **103**, 251601 (2009).
- [11] I. Selyuzhenkov (ALICE Collaboration), *Prog. Theor. Phys. Suppl.* **193**, 153 (2012).
- [12] M. Asakawa, A. Majumder, and B. Muller, *Phys. Rev. C* **81**, 064912 (2010).
- [13] A. Bzdak, V. Koch, and J. Liao, *Phys. Rev. C* **81**, 031901 (2010).
- [14] F. Wang, *Phys. Rev. C* **81**, 064902 (2010).
- [15] S. Pratt, S. Schlichting, and S. Gavin, *Phys. Rev. C* **84**, 024909 (2011).
- [16] D. E. Kharzeev and H.-U. Yee, *Phys. Rev. D* **83**, 085007 (2011).
- [17] G. M. Newman, *J. High Energy Phys.* 01 (2006) 158.
- [18] E. V. Gorbar, V. A. Miransky, and I. A. Shovkovy, *Phys. Rev. D* **83**, 085003 (2011).
- [19] Y. Burnier, D. E. Kharzeev, J. Liao, and H.-U. Yee, *Phys. Rev. Lett.* **107**, 052303 (2011).
- [20] Y. Burnier, D. E. Kharzeev, J. Liao, and H.-U. Yee, *arXiv:1208.2537*.
- [21] G. Wang (STAR Collaboration), *Nucl. Phys.* **A904–A905**, 248c (2013).
- [22] H. Ke (STAR Collaboration), *J. Phys. Conf. Ser.* **389**, 012035 (2012).
- [23] J. C. Dunlop, M. A. Lisa, and P. Sorensen, *Phys. Rev. C* **84**, 044914 (2011).
- [24] A. Bzdak and P. Bozek, *Phys. Lett. B* **726**, 239 (2013).
- [25] M. Stephanov and H.-U. Yee, *Phys. Rev. C* **88**, 014908 (2013).
- [26] W.-T. Deng and X.-G. Huang, *Phys. Rev. C* **85**, 044907 (2012).
- [27] X.-G. Huang and J. Liao, *Phys. Rev. Lett.* **110**, 232302 (2013).
- [28] R. Loganayagam, *J. High Energy Phys.* 11 (2013) 205.
- [29] A. Adare *et al.* (PHENIX Collaboration), *Phys. Rev. Lett.* **109**, 122302 (2012).
- [30] D. Lohner (ALICE Collaboration), *J. Phys. Conf. Ser.* **446**, 012028 (2013).
- [31] K. Tuchin, *Phys. Rev. C* **87**, 024912 (2013).
- [32] G. Basar, D. Kharzeev, and V. Skokov, *Phys. Rev. Lett.* **109**, 202303 (2012).
- [33] K. Fukushima and K. Mameda, *Phys. Rev. D* **86**, 071501 (2012).
- [34] A. Bzdak and V. Skokov, *Phys. Rev. Lett.* **110**, 192301 (2013).
- [35] K. A. Mamo, *J. High Energy Phys.* 08 (2013) 083.
- [36] Y. Bu, *Phys. Rev. D* **87**, 026005 (2013).
- [37] H.-U. Yee, *Phys. Rev. D* **88**, 026001 (2013).
- [38] S.-Y. Wu and D.-L. Yang, *J. High Energy Phys.* 08 (2013) 032.
- [39] B. Muller, S.-Y. Wu, and D.-L. Yang, *arXiv:1308.6568*.
- [40] S. Lin and H.-U. Yee, *Phys. Rev. D* **88**, 025030 (2013).
- [41] Y. Akamatsu and N. Yamamoto, *Phys. Rev. Lett.* **111**, 052002 (2013).
- [42] H.-U. Yee, *J. High Energy Phys.* 11 (2009) 085.
- [43] T. Sakai and S. Sugimoto, *Prog. Theor. Phys.* **113**, 843 (2005).
- [44] G. Mandal and T. Morita, *J. High Energy Phys.* 09 (2011) 073.
- [45] D. T. Son and N. Yamamoto, *Phys. Rev. Lett.* **109**, 181602 (2012).
- [46] M. A. Stephanov and Y. Yin, *Phys. Rev. Lett.* **109**, 162001 (2012).
- [47] J.-W. Chen, S. Pu, Q. Wang, and X.-N. Wang, *Phys. Rev. Lett.* **110**, 262301 (2013).